

## Solubility Enhancement of Cefdinir using different Pharmaceutical Approaches for Enhancement of the Drug Performance

Naamaa A. Naama<sup>1</sup>  , Ghaidaa S. Hameed<sup>\*1</sup>   and Dalya Basil Hanna<sup>2</sup>  

<sup>1</sup>Department of Pharmaceutics, College of Pharmacy, Mustansiriyah University, Baghdad, Iraq.

<sup>2</sup>Department of Clinical Laboratory Sciences, College of Pharmacy, Mustansiriyah University, Baghdad, Iraq.

\*Corresponding Author

Received 25/9/2023, Accepted 20/12/2023, Published 29/3/2025



This work is licensed under a Creative Commons Attribution 4.0 International License.

### Abstract

Cefdinir (CEF) is classified as a third-generation cephalosporin within class IV of the Biopharmaceutical Classification System (BCS). Consequently, it exhibits limited solubility in water, which might diminish oral bioavailability. This study aimed to compare CEF in different solubility enhancement products. Specifically, the CEF was physically mixed with co-former and then processed using different methods such as co-amorphous system formation with curcumin, binary solid dispersion (SD) with polyvinylpyrrolidone k30 (PVP), and with soluplus and ternary solid dispersion with curcumin and PVP using the solvent evaporation method. The products were subjected to characterization using Differential Scanning Calorimetry (DSC), Powder X-ray Diffractometry (PXRD), and Fourier Transform Infrared Spectroscopy (FTIR). Additionally, dissolution and *In vitro* antibacterial activity tests were performed on these systems. The findings indicate a decrease in crystallinity for both curcumin and soluplus binary systems. Conversely, in the case of CEF with PVP binary SD and ternary SD with curcumin, the results demonstrate the entire creation of an amorphous system, resulting in improved release and *in vitro* antibacterial properties compared to the pure drug. The presence of PVP in the solvent evaporated product in both binary and ternary products produces a miscible mix, which might correlate to this totally amorphous solid dispersed system.

**Keywords:** Cefdinir, solubility enhancement, co amorphous, polyvinylpyrrolidone k30, solid dispersion.

### Introduction

Co-amorphous and solid dispersion (SD) are among the methods that can potentially improve the pharmaceutical efficacy of substances<sup>(1)</sup>. Amorphous solid dispersions (ASDs) which contain a polymer dispersed with the drug, are more soluble due to the drug's amorphous shape and hydrophilic polymer<sup>(2)</sup>. PVP and Soluplus are excipients for solid dispersion<sup>(3)</sup>, which can change a drug's physical state from crystalline to amorphous due to their ability to increase the surface area and interact with drug molecules<sup>(4)</sup>. The co-amorphous state is an amorphous state in which drugs are blended with other drugs or low-molecular-weight compounds such as excipients<sup>(5)</sup>. Based on formulation composition, it can be divided into binary and multi-component (ternary) co-amorphous systems<sup>(6)</sup>. Previously, curcumin was employed as a co-former with favipiravir and soluplus to create a ternary solid dispersion system that improved favipiravir dissolution and antiviral activity<sup>(7)</sup>.

Third-generation cephalosporin cefdinir (CEF) inhibits bacterial cell wall formation and treats mild to moderate bacterial infections in both

gram-positive and gram-negative bacteria<sup>(8)</sup>. BCS class IV drug CEF<sup>(9)</sup> has a 1.7 hour elimination half-life<sup>(10)</sup>, and it is a weakly acidic drug<sup>(11)</sup> with a pKa of 8.70<sup>(12)</sup>. Thus, its oral bioavailability (16%–21%) is poor due to its pH-dependent water solubility<sup>(13)</sup>. Many approaches improve CEF solubility. Spray-drying (SD) and supercritical anti-solvent (SAS) micronized and amorphousized drug particles and crystalline structure<sup>(14)</sup>. Amorphization was also achieved via simple solid dispersion by solvent evaporation producing fast-disintegrating tablets<sup>(15)</sup>. CEF solubility and oral bioavailability have been improved by nanosuspension, niosomal encapsulation, and complex inclusion<sup>(9, 16, 17)</sup>. The dissolution rate was also increased by hydrophilic polymers and CEF loading on nanographene oxide sheets<sup>(18)</sup>. This study aims to prepare CEF using different solubility enhancement methods, including co amorphous system with curcumin, CEF solvent evaporation product (CEF S.E), binary solid dispersion with soluplus, CEF with PVP, and ternary solid dispersion with curcumin and PVP, to improve solubility, release, and *In vitro* antibacterial activity.

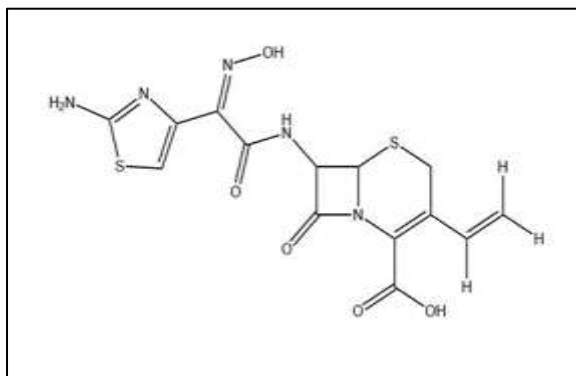


Figure 1. Cefdinir structure

## Materials and Methods

### Materials

CEF (as received) was purchased from Hubei widely Chemical Technology Co.,Ltd (China) . Polyvinylpyrrolidone K30 (PVP) was purchased from HiMedia Laboratories (India). Soluplus from

BASF pharmaceutical industries (Germany). Turmeric curcumin from Xi'an Sonwu Biotech Co.,Ltd./China. Hydrochloric acid (HCl) from Thomas Baker (Chemicals) Pvt. Ltd/India. Methanol from Sisco Research Laboratories Pvt. Ltd/India.

### Methods

#### Preparation of physical mixtures (PMs)

As seen in Table (1), first, a binary combination of CEF with curcumin, CEF with PVP, and CEF with soluplus in weight ratios of 1:1, 1:1, and 1:2 respectively was produced.

Second, a 1:1:1 ratio of CEF, curcumin, and PVP ternary combination. Both mixture components were weighed exactly and combined for five minutes in a glass mortar until a homogenous mixture was created at room temperature. For future investigation, the materials were kept in a desiccator (19, 20).

Table 1. Physical mixtures formulas (as received)

Formulation	A	B	C	D
Cefdinir	300 mg	300 mg	300 mg	300 mg
PVP	300 mg	—	—	300 mg
Soluplus	—	600 mg	—	—
Curcumin	—	—	300 mg	300 mg

#### Preparation of solid dispersion formulas (SDs)

As seen in Table (2), the amount of pure CEF, CEF and PVP in a weight ratio of 1:1, CEF and curcumin in a weight ratio of 1:1, and CEF, curcumin, and PVP in a weight ratio of 1:1:1 was dissolved in methanol then the solvent was evaporated by rotary vacuum evaporator for 30

minutes at 40 °C under reduced pressure to produce binary SD, co amorphous and ternary SD systems, respectively (20-22). While CEF and soluplus SD was prepared by milling using mortar and pestle for 30 minutes in a weight ratio of 1:2 (23). The resulting SDs were maintained in a desiccator for further characterization.

Table 2. Solid dispersion formulas

Formulation	E	F	G	H	I
Cefdinir S.E (CEF S.E)	300 mg	—	—	—	—
Cefdinir and PVP SD	—	600 mg	—	—	—
Cefdinir and soluplus SD	—	—	900 mg	—	—
Cefdinir and curcumin co amorphous	—	—	—	600 mg	—
Cefdinir, PVP and curcumin SD	—	—	—	—	900 mg

**Differential Scanning Calorimetry (DSC)**

CEF melting points were assessed by DSC<sup>(24)</sup>. A Shimadzu DSC 60 (Japan) was also used for CEF S.E, PMs, and SDs. Crimp-sealed aluminum pans (5-6 mg) held 3 mg of correctly weighed samples. The measurement was done at 10 °C/min from 35 to 280 °C<sup>(25, 26)</sup>.

**Powder X-ray Diffractometry (PXRD)**

A powder X-ray diffractometer (Aires-analytical company-Netherlands) evaluated CEF, CEF S.E, PMs, and SDs. Operating conditions: 30 mA current, 40 kV voltage, 1/min scanning speed, 10–90° (2θ) range<sup>(27)</sup>.

**Fourier Transform Infrared Spectroscopy (FTIR)**

The KBr disc technique was utilized to measure the FTIR of the CEF, CEF S.E, PMs, and SDs using a Shimadzu 8300 Fourier transform infrared system (Japan). Spectra between 4000 and 400 nm were investigated<sup>(28, 29)</sup>.

**Determination of saturated solubility**

In 0.1N HCL (PH 1.2), CEF drug as received and ternary SD saturated solubility were done in triplicate. The drug was put in an excess amount (about 25 mg) in 10 ml of buffer. Forty-eight hours of stirring at 200 rpm at 25 °C was followed by filtration through a 0.45 m syringe filter, dilution, and UV spectrophotometer analysis at 281 nm<sup>(30)</sup>.

**In vitro dissolution studies**

All dissolution investigations used a paddle (USP Apparatus II) at 37 °C. CEF, PMs, CEF S.E, and SDs were agitated at 50 rpm in 900 ml of 0.1N HCl. The trial was tripled. After 15, 30, 45, 60, and 120 min, 5 ml samples were removed using a 0.45 mm filter syringe and replenished with a new warmed (37 °C) medium to maintain volume throughout the test. Samples were measured using a UV-visible spectrophotometer at the selected λ max<sup>(31-34)</sup>.

**In vitro antibacterial activity (Determination of inhibition zone)**

The agar well diffusion technique was used to test the *In vitro* antibacterial activity of the CEF, PMs, CEF S.E, and SDs against *Staphylococcus aureus* and *Proteus vulgaris* isolates. Nutrient broth was used to cultivate isolated bacteria for 24 hours at 37 °C. The Muller-Hinton agar was prepared according to the instructions provided by the manufacturer to assess the *In vitro* antibacterial activity of the samples. Using a sterile cotton swab, transfer 100 µL of bacterial solution with a concentration of 1.5 x 10<sup>9</sup> cells/ml to each petri dish. Six mm in diameter wells were punched on the agar media using a sterile pasture pipette<sup>(35, 36)</sup>.

A volume of 1 ml of 0.1 N HCl was used to dissolve one milligram of each sample (CEF, PMs, CEF S.E, and SDs), followed by vortexing and centrifugation at 13000 RPM for five minutes. Supernatants were transferred to Muller-Hinton agar wells from

the drug as received (CEF), PMs, and SDs. The inhibition zone encircling each well was quantified 24 hours later at a temperature of 37°C.

**Results and Discussion****Differential scanning calorimetry (DSC)**

The DSC pattern of CEF, PMs, CEF S.E, and SDs are shown in Figure (2). Before processing our active ingredient, the DSC technique was used to measure the melting point of CEF, which showed a pronounced endothermic peak at 228°C. The results of Deniz Morina et al.<sup>(37)</sup>, Bohong Guo et al.<sup>(38)</sup>, and Krutika K. Sawant et al.<sup>(9)</sup> were almost similar. These endothermic peaks suggest a crystalline active ingredient.

After SE CEF showed a disappearance of melting peak with the appearance of a new wide peak at 100 that may indicate water evaporation, this result was nearly similar to previous work in which SE of cefixime showed disappearance of endothermic fusion peak at 122.1 °C, possibly related to hydrate loss during solvent evaporation<sup>(39)</sup>. After mixing with PVP, PMs showed a melting peak around 240 °C, but after solvent evaporation, the melting peak disappeared and a wide peak around 100 °C appeared; this could be related to PVP water loss, the absence of a melting peak indicates the formation of amorphous solid dispersion. The DSC of supercritical fluid-assisted carvedilol-PVP solid dispersion showed the absence of a melting point peak but a broad endothermic peak from 50 to 150 °C, which can be related to the loss of water present in the sample due to PVP's extreme hygroscopicity<sup>(40)</sup>. Mixing with soluplus resulted in a melting peak of about 240 °C, but following solvent evaporation, the peak vanished and a broad peak developed around 100 C°, indicating amorphous formation. Wide peak may be attributed to soluplus's hygroscopicity and water loss<sup>(41)</sup>.

By mixing with curcumin, the physical mixture exhibits an endothermic peak around 182 C° which corresponds to curcumin as mentioned before by Wenling Fan et al.<sup>(42)</sup> and CEF melting point respectively, after solvent evaporation there is no change in the thermogram. In the ternary mixture, two peaks at 182 °C and 228 °C correspond to curcumin and CEF melting points, respectively. After solvent evaporation, these peaks disappeared, with the appearance of a wide peak at 100 C°, indicating amorphous system formation. Similar results were obtained from ternary SD of gefitinib (ZD) with different ratios of PVP or HPMC and Eudragit S 100 generated by spray drying (SD), DSC showed that the ZD melting peak was completely missed and replaced with a broad peak in all solid dispersions thermograms, indicating successful drug conversion into its amorphous form<sup>(43)</sup>.

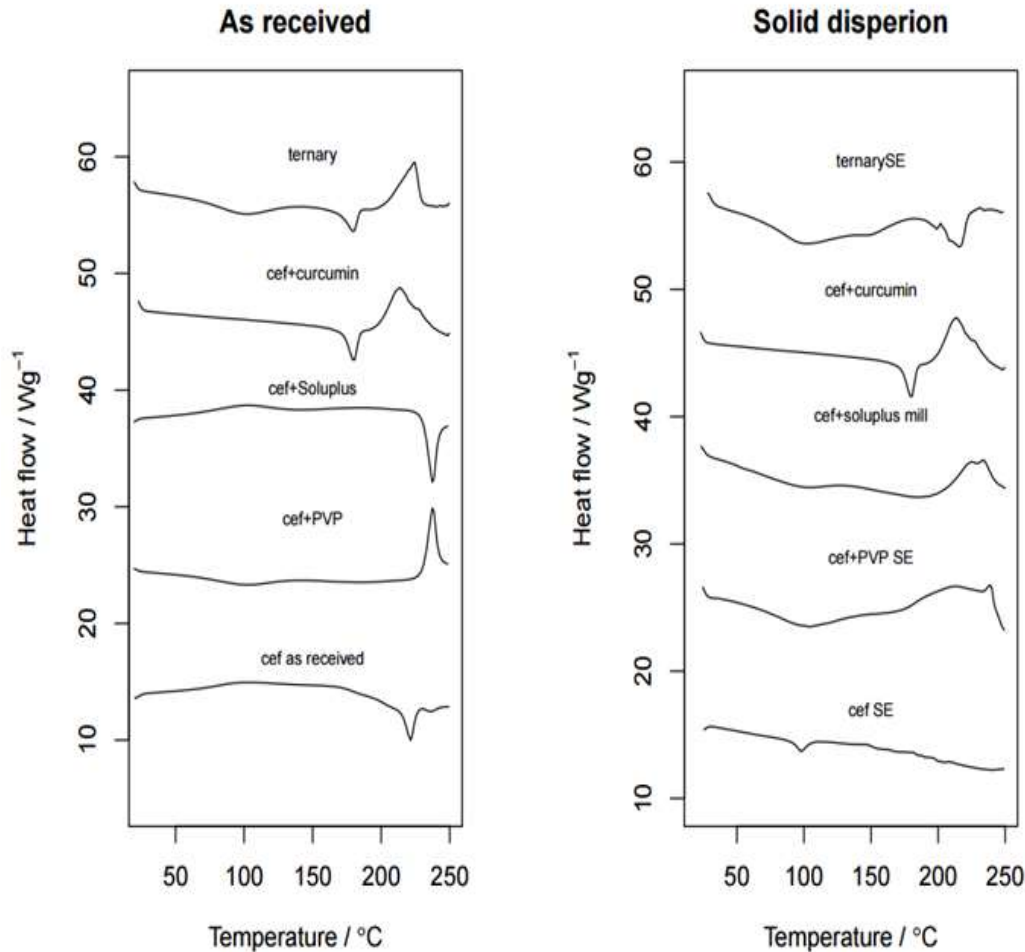


Figure 2. DSC thermograms of CEF, PMs as received and SDs.

#### Powder X-ray diffraction (PXRD)

The PXRD pattern of CEF, PMs, CEF S.E, and SDs are shown in Figure (3). The PXRD patterns of the pure drug showed several peaks at  $2\theta$  angles in the Bragg's peaks, confirming the crystalline nature of CEF, as previously reported<sup>(37)</sup>. In the case of binary mixtures of CEF and curcumin, CEF and soluplus, CEF and PVP and a ternary mixture of CEF, curcumin and PVP Bragg's peaks remain visible with slight intensity variations, indicating crystalline composition. Excipients may have diluted drug peaks in the PM, causing these intensity changes<sup>(13)</sup>. Bragg's peaks reduce with CEF solvent evaporation, indicating the drug may lose some of its crystallinity and return to semi-crystalline form, as seen in a previous study for

azithromycin<sup>(39)</sup>. On the other hand, the binary SD system of CEF and curcumin, CEF and soluplus exhibited a decline in intensities of CEF Bragg's peaks, suggesting that most of CEF were transformed to an amorphous state. In the case of the binary SD system of CEF with PVP, and ternary SD system of CEF, curcumin, and PVP the sharp peaks were missing and amorphous halo peaks appeared, indicating a full transition of cefdinir from crystalline to amorphous to create SD and ternary SD. This shows that the hydrophilic polymer (PVP) can convert cefdinir from crystalline to amorphous form<sup>(44, 45)</sup>. These are identical to the results obtained from DSC that indicate amorphous formation.

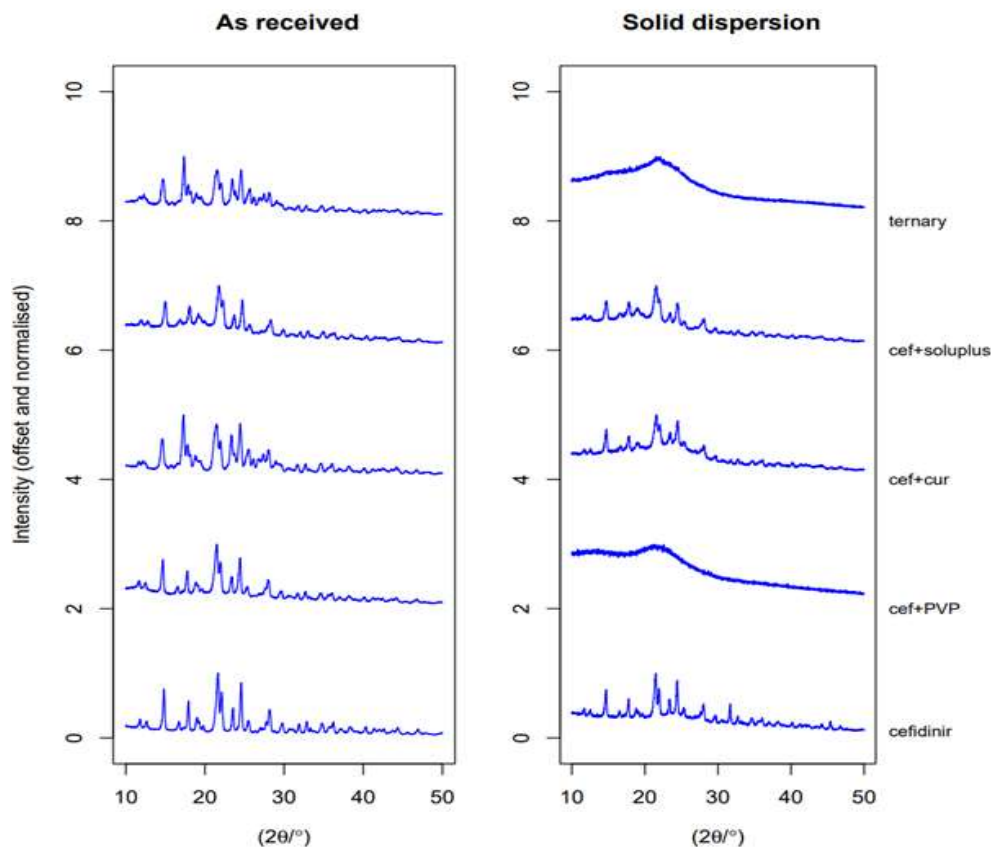


Figure 3. PXRD patterns of CEF, PMs as received, and SDs.

#### Fourier Transform Infrared Spectroscopy (FTIR)

As seen in Figure (4), Table (3) FTIR spectrum of CEF shows N-H stretching at  $3360\text{ cm}^{-1}$ , O-H stretching of the carboxyl group at  $3298.28$  and  $3059.1\text{ cm}^{-1}$ , and C-H stretching at  $2939.52$  and  $2873.94\text{ cm}^{-1}$ . A similar CEF spectral pattern has been reported<sup>(38)</sup>.

The FTIR spectra of the PMs and the pure drug did not significantly vary from one another. Drug solvent evaporation (CEF S.E) caused N-H stretch absorption to move from  $3360\text{ cm}^{-1}$  to  $3350\text{ cm}^{-1}$  and widen the peak. Such shift may indicate changes in intermolecular hydrogen bonding owing to CEF semi-crystalline conversion. The shift in CEF characteristic peaks indicates hydrogen bonding between SD components in binary SDs (CEF and PVP, CEF and soluplus, and CEF and curcumin). This is consistent with previous research on

resveratrol by forming solid dispersions using Eudragit® E PO, polyethylene glycol 6000 (PEG 6000), Kollidon® 30 (PVP K30), and Soluplus®, where shifting and disappearing in peaks indicate hydrogen bond formation<sup>(46)</sup>. In ternary SD of CEF, curcumin, and PVP, the peak for cefdinir's -NH (at  $3360\text{ cm}^{-1}$ ) was absent, while CEF's -OH stretching changed from  $3298.28$  and  $3059.1\text{ cm}^{-1}$  to  $3302.13$  and  $3116.97\text{ cm}^{-1}$  respectively. -NH peak vanished and -OH shift in the SD system, suggesting intermolecular hydrogen bonds and amorphous formation. Results were consistent with Jinfeng Chen et al.'s findings that when simvastatin co-amorphized with epigallocatechin-3-gallate (EGCG), the OH peak at  $3551\text{ cm}^{-1}$  disappeared and the -C=O stretching of SIM shifted, indicating that intermolecular hydrogen bonds formed in the co-amorphous system<sup>(47)</sup>.

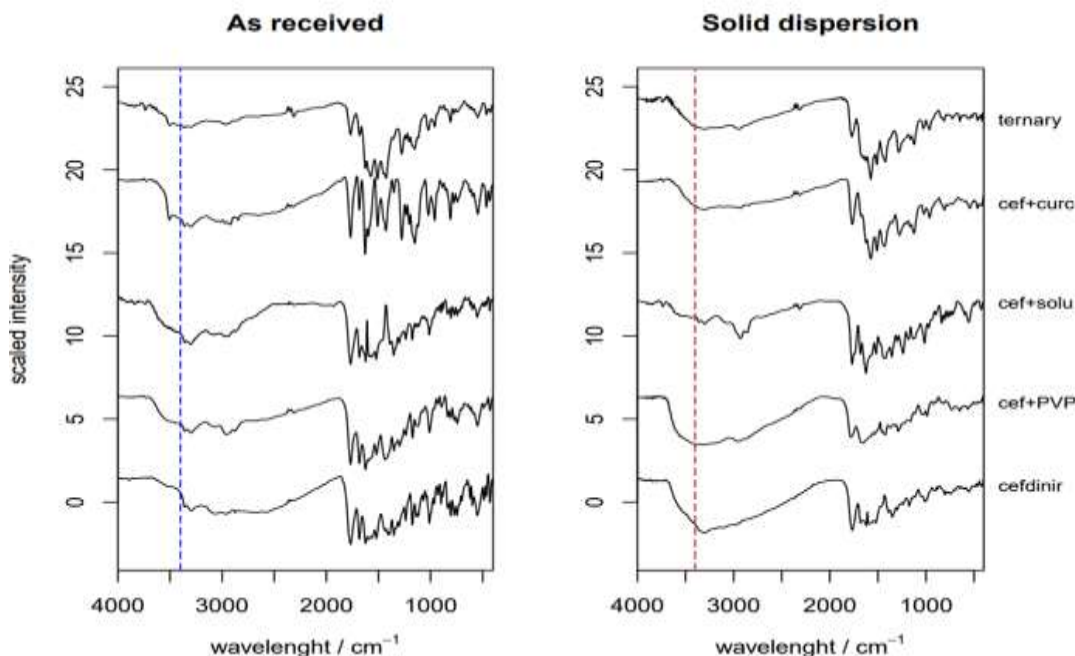


Figure 4. FTIR patterns of CEF, PMs as received, and SDs.

Table 3. FTIR spectra of Cefdinir in all Cefdinir containing formula

As received (PMs)					
Group	Pure CEF	PM CEF+PVP	PM CEF+solu	PM CEF+cur	PM ternary
N-H	3360	3360	3360	3360	3360
O-H	3298.28	3298.28	3302.13	3298.28	3298.28
	3059.1	3059.1	3028.25	3059.1	3059.1
N-H bending	1519.91	1519.91	1519.91	1508.33	1508.33
Solvent evaporated (SDs)					
Group	CEF SE	CEF+PVP SD	CEF+solu SD	CEF+cur coamorphous	Ternary SD
N-H	3350	Dis	3360	3352	Dis
O-H	3302.13	3321.42	3298.28	3302.13	3302.13
	3116.97	3116.97	3062.96	3116.97	3116.97
N-H bending	1523.76	1539.2	1519.91	1508.33	1508.33

#### Determination of saturated solubility

Table (4) shows pure drug (CEF as received) and ternary SD formulation saturated solubility in 0.1N HCl. Compared to CEF, SDs formula has much higher solubility. The drug's full transition from crystalline to amorphous, as shown by DSC and XRPD, and molecular dispersion in the hydrophilic carrier increase its solubility. Previous research supported this finding<sup>(44)</sup>.

Table 4. Saturated solubility study of pure drug and ternary SD

Formulation	Saturation solubility (mg/ml)
CEF as received	1.76523 ± 0.21
Ternary SD	4.701337 ± 0.30

#### In vitro dissolution studies

As seen in Figure (5), about 46.87 percent of CEF dissolves in 120 minutes. The dissolving rate increased to 73.48%, 50.69%, and 59.03% in binary PMs of CEF and PVP, CEF and soluplus, and CEF and curcumin respectively. For CEF, PVP, and curcumin ternary PM, the dissolution rate was about (100 %). The solvent evaporation of the CEF (CEF S.E) dissolution profile was improved (73% of the drug dissolved in 120 minutes). The dissolution rate of CEF and PVP SD, CEF, and soluplus SD was 76.5 % and 47.32 %, respectively, while the rate of CEF and curcumin co-amorphous was 3.2 %. This dramatic decline in CEF dissolution rate compared to crystalline drug may be due to aggregation during dissolution. This result is consistent with Jiawei Han et al., who found that a co-amorphous curcumin-magnolol (CUR-MAG CM) system, compared to its

crystalline counterparts, showed decreased dissolution due to aggregation. Here, HPMC, HPC, and PVP K30 were co-formulated with CUR-MAG CM to create ternary co-amorphous systems that dissolved faster and better than crystalline<sup>(48)</sup>. The dissolution rate of ternary SD of CEF, PVP, and curcumin is increased by 100% in 120 minutes. This is possible because of the development of ternary SD, which enhances the drug dissolution rate, which

is consistent with prior studies showing that PVP/resveratrol solid dispersions had increased apparent solubility and almost fully released the drug after 30 minutes<sup>(49)</sup>. Also, in another study, they reported that solubility enhancement of ibuprofen drug could be achieved by ternary amorphous system formation (ibuprofen, PVP,  $\beta$ -cyclodextrin)<sup>(50)</sup>.

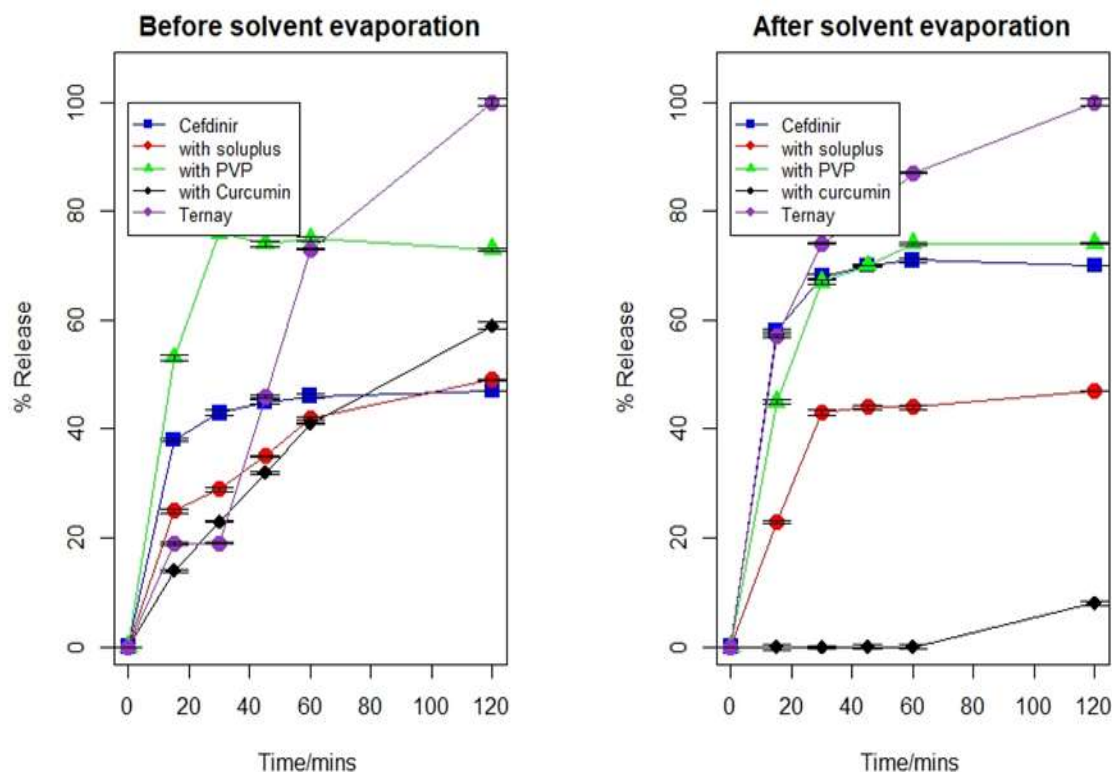


Figure 5. Dissolution profile of CEF, PMs as received and SDs.

#### *In vitro* antibacterial activity (Determination of inhibition zone)

Agar well diffusion tests showed that all drug samples tested (CEF, PMs, CEF S.E, and SDs) were active against *Staphylococcus aureus* and *Proteus vulgaris* bacterial isolates. The inhibitory zone of CEF against *Staphylococcus aureus* became larger only in the case of CEF, curcumin, and PVP ternary SD formula when compared to the CEF, as seen in Figures (6), while all PMs and SDs formulas have a larger zone of inhibition against *proteus vulgaris* compared to the CEF as seen in Figures (7). Increased drug solubility in prepared formulas may explain the increase in the *In vitro* antibacterial activity<sup>(51)</sup>. An increase in the drug's permeability across the cell membrane might be another factor enhancing the *In vitro* antibacterial

activity<sup>(52)</sup>. The differences in antimicrobial properties may be due to the membrane characteristics and wall structure of Gram-negative (*Proteus vulgaris*) bacteria, which have a thinner peptidoglycan layer than Gram-positive bacteria; this allows cefdinir formulas to easily destabilize and break down bacterial cell walls. Therefore, we observed a strong antibacterial action of CEF formulas against Gram-negative bacteria. This is in agreement with a previous study that developed hard-cellulose capsules containing cefpodoxime proxetil (CFD) (BCS Class II) loaded novel PluronicVR F127 (P127)/Polyvinylpyrrolidone K30 (PVP) solid dispersions (SDs), which showed significantly higher antibacterial activity against Gram-negative and Gram-positive bacteria than pure CFD<sup>(53)</sup>.

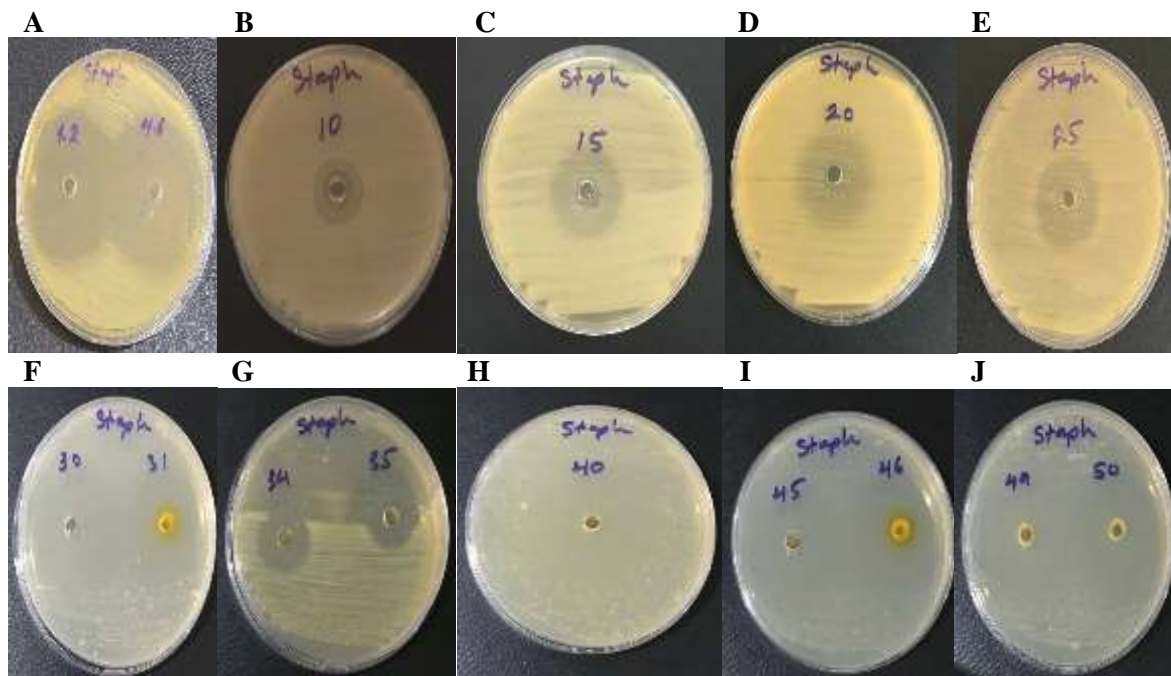


Figure 6. The inhibition zone against *Staphylococcus aureus* of A- (1.2) pure CEF, B- CEF and soluplus SD, C- PM of CEF and soluplus, D- PM of CEF and PVP, E- CEF and PVP SD, F- (30) pure CEF SE, G- (35) PM of ternary system, H- ternary SD, I- (45) PM of CEF and curcumin, J- (50) CEF and curcumin SD.

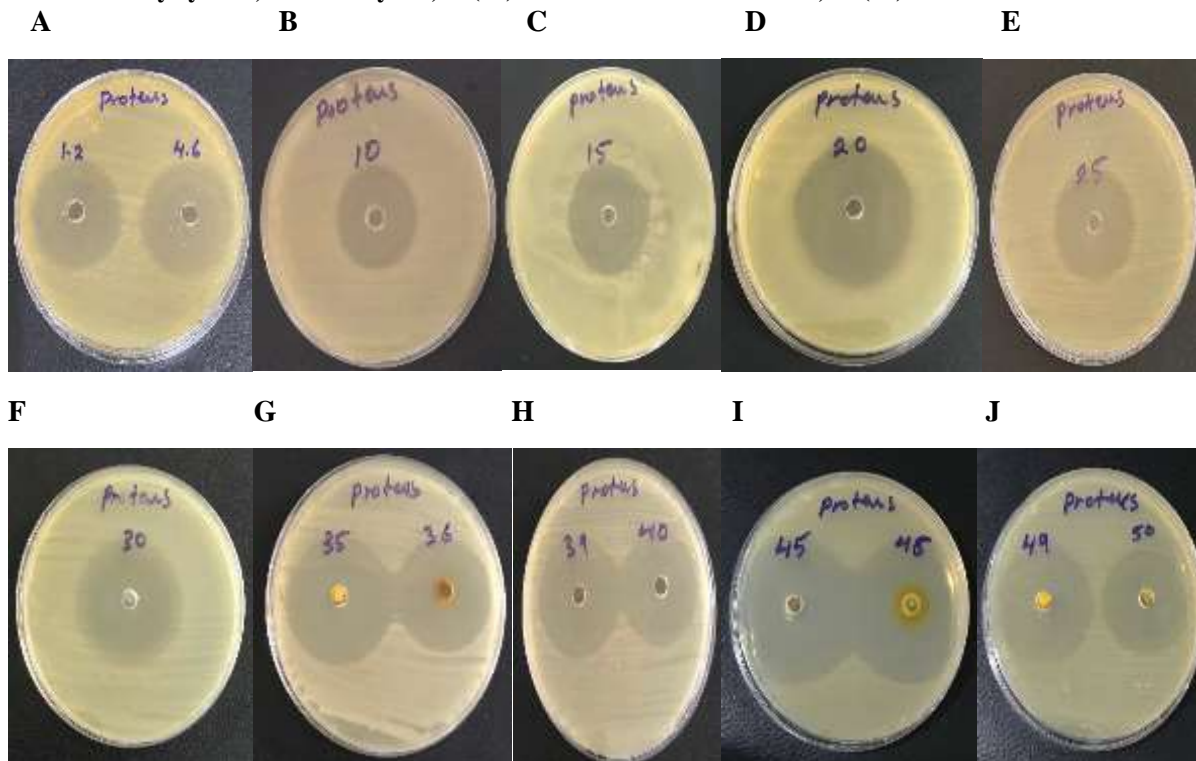


Figure 7. The inhibition zone against *Proteus vulgaris* of A- (1.2) pure CEF, B- CEF and soluplus SD, C- PM of CEF and soluplus, D- PM of CEF and PVP, E- CEF and PVP SD, F- pure CEF SE, G- (35) PM of ternary system, H- (40) ternary SD, I- (45) PM of CEF and curcumin, J- (50) CEF and curcumin SD.

## Conclusion

This work created co-amorphous, binary, and ternary SD CEF solubility enhanced products. PVP in the solvent evaporated products in both binary and ternary products creates a miscible mix that may lead to the formation of a totally amorphous solid dispersed system, which increases drug dissolution rate and *In vitro* antibacterial activity. This can be used in future work to modify CEF's physical properties and dissolution rate.

## Acknowledgment

The authors express acknowledge to the Department of Pharmaceutics- College of Pharmacy/ Mustansiriyah University (Baghdad, Iraq) for providing the support and facilities to carry out the investigation

## Conflicts of Interest

The authors have no conflicts of interest regarding this investigation.

## Funding

The author declare that they have no funding support for this study.

## Ethics Statements

This research did not use in vivo study.

## Author Contribution

Study conception and design: Naama A. Naama, Ghaidaa S. Hameed, Dalya Basil Hanna; data collection: Naama A. Naama; analysis and interpretation of results: Naama A. Naama, Ghaidaa S. Hameed, Dalya Basil Hanna; draft manuscript preparation: Naama A. Naama. All authors reviewed the results and approved the final version of the manuscript.

## References

1. Kiyonga EM, Kekani LN, Chidziwa TV, Kahwenga KD, Bronkhorst E, Milne M, et al. Nano-and Crystal Engineering Approaches in the Development of Therapeutic Agents for Neoplastic Diseases. *Crystals*. 2022;12(7):926.
2. Tran P, Pyo Y-C, Kim D-H, Lee S-E, Kim J-K, Park J-S. Overview of the manufacturing methods of solid dispersion technology for improving the solubility of poorly water-soluble drugs and application to anticancer drugs. *Pharmaceutics*. 2019;11(3):132.
3. Sarpal K, Munson EJ. Amorphous solid dispersions of felodipine and nifedipine with Soluplus®: drug-polymer miscibility and intermolecular interactions. *Journal of Pharmaceutical Sciences*. 2021;110(4):1457-69.
4. Song B, Wang J, Lu SJ, Shan LN. Andrographolide solid dispersions formulated by Soluplus to enhance interface wetting, dissolution, and absorption. *Journal of Applied Polymer Science*. 2020;137(6):48354.
5. Mizoguchi R, Waraya H, Hirakura Y. Application of co-amorphous technology for improving the physicochemical properties of amorphous formulations. *Molecular pharmaceutics*. 2019;16(5):2142-52.
6. Fang X, Hu Y, Yang G, Shi W, Lu S, Cao Y. Improving physicochemical properties and pharmacological activities of ternary co-amorphous systems. *European Journal of Pharmaceutics and Biopharmaceutics*. 2022;181:22-35.
7. Hashim G, Hameed G, Hanna D. Improving the Dissolution Rate and the Bioavailability of Favipiravir by Solid Dispersion with Curcumin. *Latin American Journal of Pharmacy*. 2023:68-76.
8. Dinç E, Dermiş S, Can Akcasoy S, Ceren Ertekin Z. A New Chemometric strategy in electrochemical method optimization for the quantification of cefdinir in tablets, effervescent tablets and suspension samples. *Electroanalysis*. 2020;32(3):613-9.
9. Sawant KK, Patel MH, Patel K. Cefdinir nanosuspension for improved oral bioavailability by media milling technique: formulation, characterization and in vitro-in vivo evaluations. *Drug development and industrial pharmacy*. 2016;42(5):758-68.
10. Al Okla S, Prashanth GP, Kurbet S, Al Attraqchi Y, Asaad A. Emergent "Bloody Diarrhea" Associated with the Use of Oral Cefdinir in Young Children: A Brief Report and Review of Literature. *The Journal of Emergency Medicine*. 2023.
11. Al Nuss R. pH-Modified Solid Dispersions of Cefdinir for Dissolution Rate Enhancement: Formulation and Characterization. *J Pharm Nutr Sci*. 2021;11:101-15.
12. Al-Badr AA, Alasseiri FA. Cefdinir. Profiles of Drug Substances, Excipients and Related Methodology. 2014;39:41-112.
13. Jung D-H, Song JG, Han H-K. Development and evaluation of a sustained release solid dispersion of cefdinir using a hydrophobic polymeric carrier and aminoclay. *Journal of Drug Delivery Science and Technology*. 2023;84:104503.
14. Park J, Park HJ, Cho W, Cha K-H, Kang Y-S, Hwang S-J. Preparation and pharmaceutical characterization of amorphous cefdinir using spray-drying and SAS-process. *International journal of pharmaceutics*. 2010;396(1-2):239-45.
15. Jain S, Jain S, Mishra A, Garg G, Modi RK. Formulation and characterization of fast disintegrating tablets containing Cefdinir solid dispersion. *International Journal of Pharmacy & Life Sciences*. 2012;3(12).
16. Bansal S, Aggarwal G, Chandel P, Harikumar S. Design and development of cefdinir niosomes for oral delivery. *Journal of pharmacy & bioallied sciences*. 2013;5(4):318.
17. Aleem O, Kuchekar B, Pore Y, Late S. Effect of  $\beta$ -cyclodextrin and hydroxypropyl  $\beta$ -

- cyclodextrin complexation on physicochemical properties and antimicrobial activity of cefdinir. *Journal of pharmaceutical and biomedical analysis*. 2008;47(3):535-40.
18. Bali DE, Arafa MF, Gamaleldin NM, El Maghraby GM. Nanographene oxide for enhanced dissolution rate and antibacterial activity of cefdinir. *Journal of Drug Delivery Science and Technology*. 2021;62:102411.
  19. Leonardi D, Salomon CJ. Unexpected performance of physical mixtures over solid dispersions on the dissolution behavior of benznidazole from tablets. *Journal of pharmaceutical sciences*. 2013;102(3):1016-23.
  20. Arora S, Sharma P, Irchhaiya R, Khatkar A, Singh N, Gagoria J. Development, characterization and solubility study of solid dispersions of cefuroxime axetil by the solvent evaporation method. *Journal of Advanced Pharmaceutical Technology & Research*. 2010;1(3):326.
  21. Douroumis D, Bouropoulos N, Fahr A. Physicochemical characterization of solid dispersions of three antiepileptic drugs prepared by solvent evaporation method. *Journal of pharmacy and pharmacology*. 2007;59(5):645-53.
  22. Tabbakhian M, Hasanzadeh F, Tavakoli N, Jamshidian Z. Dissolution enhancement of glibenclamide by solid dispersion: solvent evaporation versus a supercritical fluid-based solvent-antisolvent technique. *Research in pharmaceutical sciences*. 2014;9(5):337.
  23. Panghal D, Nagpal M, Thakur GS, Arora S. Dissolution improvement of atorvastatin calcium using modified locust bean gum by the solid dispersion technique. *Scientia pharmaceutica*. 2014;82(1):177-92.
  24. Leyva-Porras C, Cruz-Alcantar P, Espinosa-Solís V, Martínez-Guerra E, Piñón-Balderrama CI, Compean Martínez I, et al. Application of differential scanning calorimetry (DSC) and modulated differential scanning calorimetry (MDSC) in food and drug industries. *Polymers*. 2019;12(1):5.
  25. Ali SK, Al-Khedairy EB. Solubility and dissolution enhancement of atorvastatin calcium using solid dispersion adsorbate technique. *Iraqi J Pharm Sci*. 2019;28(2):105-14.
  26. Abd-AllRazaq IF, Rahi FA, Al-lami MS. Preparation And Characterization Of Nimesulide Nanoparticles For Dissolution Improvement. *Al Mustansiriyah Journal of Pharmaceutical Sciences*. 2018;18(1):46-60.
  27. Jaiswar DR, Jha D, Amin PD. Preparation and characterizations of stable amorphous solid solution of azithromycin by hot melt extrusion. *Journal of Pharmaceutical Investigation*. 2016;46:655-68.
  28. Rao MR, Chaudhari J, Trotta F, Caldera F. Investigation of cyclodextrin-based nanosponges for solubility and bioavailability enhancement of rilpivirine. *Aaps Pharmscitech*. 2018;19:2358-69.
  29. Tawfeeq TA, Jasim GA, Nasser AA. Isolation of umbelliferone from leaves of *Conocarpus erectus* L. cultivated in Iraq. *Al Mustansiriyah Journal of Pharmaceutical Sciences*. 2020;20(4):82-92.
  30. Nagaraj K, Narendar D, Kishan V. Development of olmesartan medoxomil optimized nanosuspension using the Box–Behnken design to improve oral bioavailability. *Drug development and industrial pharmacy*. 2017;43(7):1186-96.
  31. Gadhiya DT, Patel JK, Bagada AA. An impact of nanocrystals on dissolution rate of Lercanidipine: Supersaturation and crystallization by addition of solvent to antisolvent. *Future Journal of Pharmaceutical Sciences*. 2021;7:1-17.
  32. Gray V, Kelly G, Xia M, Butler C, Thomas S, Mayock S. The science of USP 1 and 2 dissolution: present challenges and future relevance. *Pharmaceutical research*. 2009;26:1289-302.
  33. Praveen R, Verma PRP, Singh SK, George JK. Cross linked alginate gel beads as floating drug delivery system for cefdinir: optimization using Box–Behnken design. *Journal of pharmaceutical investigation*. 2015;45:187-99.
  34. Malik MM, Maraie NK. Preparation and evaluation of famotidine nanosuspension. *Al Mustansiriyah Journal of Pharmaceutical Sciences*. 2018;18(2):13-23.
  35. Alhasan DA. In Vitro Antimicrobial Activity of Curcumin-Copper Complex. *University of Thi-Qar Journal*. 2021;16(1):73-97.
  36. Ali ZA, Jasim TM, Alani WM. Antibacterial activity of chloroform extract from *Tagetes Erecta* L. flowers. *Al Mustansiriyah Journal of Pharmaceutical Sciences*. 2019;19(4):7-15.
  37. Morina D, Sessevmez M, Sinani G, Mülazımoğlu L, Cevher E. Oral tablet formulations containing cyclodextrin complexes of poorly water soluble cefdinir to enhance its bioavailability. *Journal of Drug Delivery Science and Technology*. 2020;57:101742.
  38. Guo B, Zhong S, Li N, Li X, Yi J, Jin M. Dissolution enhancement of cefdinir with hydroxypropyl- $\beta$ -cyclodextrin. *Drug Development and Industrial Pharmacy*. 2013;39(11):1638-43.
  39. ISMAEL QA, HAMEED GS, AZIZ FM. Effect of Introduction of Polymers on the Antibacterial Activity of Crystalline Antibiotics. *International Journal of Pharmaceutical Research (09752366)*. 2020;12(3).

40. Djuris J, Milovanovic S, Medarevic D, Dobricic V, Dapčević A, Ibric S. Selection of the suitable polymer for supercritical fluid assisted preparation of carvedilol solid dispersions. *International journal of pharmaceutics*. 2019;554:190-200.
41. Nowak P, Krupa A, Kubat K, Węgrzyn A, Harańczyk H, Ciułkowska A, et al. Water vapour sorption in tadalafil-Soluplus co-milled amorphous solid dispersions. *Powder Technology*. 2019;346:373-84.
42. Fan W, Zhu W, Zhang X, Di L. The Preparation of Curcumin Sustained-Release Solid Dispersion by Hot Melt Extrusion—I. Optimization of the Formulation. *Journal of Pharmaceutical Sciences*. 2020;109(3):1242-52.
43. Mustafa WW, Fletcher J, Khoder M, Alany RG. Solid dispersions of gefitinib prepared by spray drying with improved mucoadhesive and drug dissolution properties. *AAPS PharmSciTech*. 2022;23(1):48.
44. Cho H-J, Jee J-P, Kang J-Y, Shin D-Y, Choi H-G, Maeng H-J, et al. Cefdinir solid dispersion composed of hydrophilic polymers with enhanced solubility, dissolution, and bioavailability in rats. *Molecules*. 2017;22(2):280.
45. Choi J-S, Park J-S. Design of PVP/VA S-630 based tadalafil solid dispersion to enhance the dissolution rate. *European journal of pharmaceutical sciences*. 2017;97:269-76.
46. Yu C, Zhang C, Guan X, Yuan D. The solid dispersion of resveratrol with enhanced dissolution and good system physical stability. *Journal of Drug Delivery Science and Technology*. 2023;84:104507.
47. Chen J, Li H, Li X, Yuan D, Cheng H, Ke Y, et al. Co-amorphous systems using epigallocatechin-3-gallate as a co-former: Stability, in vitro dissolution, in vivo bioavailability and underlying molecular mechanisms. *European Journal of Pharmaceutics and Biopharmaceutics*. 2022;178:82-93.
48. Han J, Li L, Su M, Heng W, Wei Y, Gao Y, et al. Deaggregation and crystallization inhibition by small amount of polymer addition for a co-amorphous curcumin-magnolol system. *Pharmaceutics*. 2021;13(10):1725.
49. Wang B, Wang D, Zhao S, Huang X, Zhang J, Lv Y, et al. Evaluate the ability of PVP to inhibit crystallization of amorphous solid dispersions by density functional theory and experimental verify. *European Journal of Pharmaceutical Sciences*. 2017;96:45-52.
50. Bejaoui M, Galai H, Amara ABH, Ben Rhaïem H. Formation of water soluble and stable amorphous ternary system: ibuprofen/ $\beta$ -cyclodextrin/PVP. *Glass Physics and Chemistry*. 2019;45:580-8.
51. Mendes C, Valentini G, Chamorro Rengifo AF, Pinto JM, Silva MA, Parize AL. Supersaturating drug delivery system of fixed drug combination: sulfamethoxazole and trimethoprim. Expert review of anti-infective therapy. 2019;17(10):841-50.
52. Mesallati H, Umerska A, Paluch KJ, Tajber L. Amorphous polymeric drug salts as ionic solid dispersion forms of ciprofloxacin. *Molecular pharmaceutics*. 2017;14(7):2209-23.
53. Yurtdaş-Kırımıoğlu G. Development and characterization of lyophilized cefpodoxime proxetil-Pluronic® F127/polyvinylpyrrolidone K30 solid dispersions with improved dissolution and enhanced antibacterial activity. *Pharmaceutical Development and Technology*. 2021;26(4):476-89.

## تحسين قابلية ذوبان السيفدينير باستخدام طرق صيدلانية مختلفة لتحسين الأداء الدوائي

نعماء عدنان نعمة<sup>1</sup>، غيداء سليمان حميد<sup>1\*</sup> و داليا باسل حنا<sup>2</sup>

<sup>1</sup> فرع الصيدلانيات، كلية الصيدلة، الجامعة المستنصرية، بغداد، العراق.

<sup>2</sup> فرع العلوم المخبرية السريرية، كلية الصيدلة، الجامعة المستنصرية، بغداد، العراق.

### الخلاصة

يتم تصنيف سيفدينير باعتباره الجيل الثالث من السيفالوسبورينات ضمن الفئة الرابعة من نظام تصنيف الأدوية الحيوية. ونتيجة لذلك، فإنه يظهر قابلية ذوبان محدودة في الماء، مما قد يقلل من التوافر البيولوجي عن طريق الفم. تهدف هذه الدراسة إلى مقارنة السيفدينير في مختلف منتجات تعزيز الذوبان على وجه التحديد تم خلط السيفدينير مع المادة المشاركة ومن ثم معالجتها باستخدام طرق مختلفة مثل تكوين النظام غير المتبلور المشترك مع الكركمين والتشتت الصلب الثنائي مع البوليفينيل بيروليدين ومع السولوبليس والتشتت الصلب الثلاثي مع الكركمين والبوليفينيل بيروليدين باستخدام طريقة التبخير بالمذيبات. تم إخضاع المنتجات للتوصيف باستخدام المسح التفاضلي المسعر، وقياس انحراف الأشعة السينية بالمسحوق، وتحويل فورييه الطيفي للأشعة تحت الحمراء بالإضافة إلى ذلك، تم إجراء اختبارات الذوبان والنشاط المضاد للبكتيريا على هذه الأنظمة. تشير النتائج إلى انخفاض في التبلور لكل من النظامين الثنائي مع الكركمين ومع السولوبليس على العكس من ذلك، في حالة التشتت الصلب الثنائي مع البوليفينيل بيروليدين والتشتت الصلب الثلاثي، توضح النتائج الإنشاء الكامل لنظام غير متبلور، مما يؤدي إلى تحسين الإطلاق والخصائص المضادة للبكتيريا مقارنة بالدواء النقي. يؤدي وجود البوليفينيل بيروليدين في المنتج المخبر بالمذيب في كل من المنتج الثنائي والثلاثي إلى إنتاج مزيج قابل للامتزاج والذي قد يرتبط بالإنشاء الكامل لنظام غير متبلور.

الكلمات المفتاحية: سيفدينير، تعزيز الذوبان، غير المتبلور المشترك، البوليفينيل بيروليدين، تشتت صلب